Anal. Bioanal. Electrochem., Vol. 12, No. 5, 2020, 653-662

Analytical& Bioanalytical Electrochemistry

2020 by CEE
www.abechem.com

Full Paper

Manganese Ferrite Nanocomposite Modified Electrochemical Sensor for the Detection of Guanine and Uric Acid

Yogendra Kumar, Vinod Kumar Vashistha,* Vivek Sharma, Rahul Patil, and Dipak Kumar Das*

**Department of Chemistry, GLA University, Mathura, 281406 India*

*Corresponding Author, Tel: 09927223500, Fax: 05662-241687

E-Mail: deepak.das@gla.ac.in; vinod.vashistha@gla.ac.in

Received: 21 March 2020 / Received in revised form: 16 May 2020 / Accepted: 18 May 2020 / Published online: 31 May 2020

Abstract- Manganese ferrite nanoparticles were produced by applying the combustion technique using the manganese acetate and ferric nitrate as the starting material. Analytical techniques like FESEM and TEM were utilized to characterize the synthesized materials. The typical size was observed in the range of 12 to 14 nm with a cubic structure. The synthesized material was used as an electrochemical sensor which was fabricated using the nanocomposite for the identification of guanine (GU) and uric acid (UA) (individually and in their mixture). The cyclic voltammeter and differential pulse voltammeter techniques were deployed to check the sensor activity of the modified electrode. Lower detection limit for GU and UA was found to be 400 nM and 450 nM, with linearity range 0.5 to 120 µM and 02 to 140 µM for GU and UA respectively. The electrochemical sensor developed in this method can be widely employed for the identification of GU and UA and analogs in biofluids or dosage forms.

Keywords- Electrocatalyst; Nanocomposite; Manganese ferrite nanocomposite; Electrochemical sensor; Guanine; Uric acid

1. INTRODUCTION

A naturally occurring biogenic compound, generated in the “Dargic neurons”. In the ventricular part of the midbrain, known as the Dopamine (DA) [4-(2-aminoethyl) benzene-

1,2-diol] which are strongly engaged in mechanisms in the brain like the actions of learning, motion control, thinking and cognition. During the physical activities, it mediates functions of the central and peripheral nervous system [1,2] and is also accountable for the endocrine system and emotion. A small congregation of DA can cause "mouth burning syndrome" [3], "restless leg syndrome" [4], "senile dementia", "fibromyalgia" [5,6], and "rarely depression" [7]. The reduction of DA in the cerebellar zone can produce "Parkinson's disease" [8]. Cocaine, heroin, nicotine, etc. intake elevates the DA congregation resulting in unusual BP and heart rate augmentation. The predictable technique being expensive, cheap, and delicate electrode to detect biomolecules at low concentration is therefore essential. Hence, due to edges such as quick retort, finer selectivity, high sensitivity, and small cost, the electrochemical techniques received tremendous attention from researches for the last few decades. Several electrode materials like Co-doped CeO_2 nanoparticles (nps) [9], MWCNT-Fe_3O_4@PDA-Ag nanocomposite [10], nitrogen-doped graphene nps [11], reduced graphene oxide [12], nickel telluride and cobalt telluride nps [13], PbTe/GP electrode [14], glassy carbon electrode fabricated with zinc oxide [15], lanthanide- ortho-ferrites & cobalt ferrite/ manganese ferrite nps [16-18], and urease immobilized biosensor [19] have been used as electrode modifier. Herein, we report the simple synthesis method of manganese ferrite nanoparticles and their uses as electrode modifier with graphite powder to prepare an electrode to detect guanine (GU) and uric acid (UA) individually and in mixture with the help of cyclic voltammeter (CV) and differential pulse voltammetry (DPV) techniques.

2. MATERIALS AND METHODS

2.1. Chemical and Reagents

Manganese acetate, iron nitrate, HNO_3, paraffin oil, and ethanolamine were purchased from Merck (India) and graphite flakes, uric acid ($C_5H_4N_4O_3$), guanine ($C_5H_5N_5O$), etc. were procured from Sigma Aldrich, USA. Analytical grade reagents were used as such and double distilled water being used for solutions. The percentage purity of all compounds was ≥ 99%.

2.2. Synthesis of Manganese ferrite nanoparticles

Synthesis of the manganese ferrite nps was carried out by following the procedure described in the literature [20,21]. Manganese acetate (1.0 mM) was taken in a 1000 ml beaker having 100 ml double distilled water and ferric nitrate (2.0 mM), nitric acid (3.5 mM), mono-ethanolamine (1.7 mM) and sugar (2.5 mM) were mixed in it. The resultant mixture was heated at 150 ^oC till dryness. After combustion, a blackish fluffy mass obtained was ground with the help of pastel and calcined at 600 ^oC for 6 hours to get nanoparticles of manganese ferrite. The schematic diagram for the synthesis of manganese ferrite nps is present in Fig. 1.

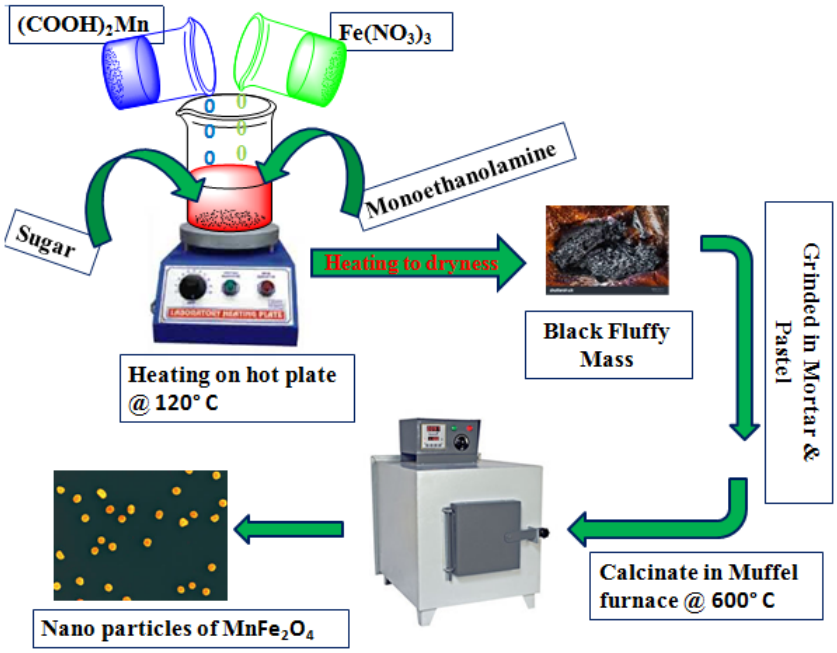

Fig. 1. Synthesis procedure of $MnFe_2O_4$ nanoparticles

2.3. Electrodes preparation

Graphite powder and prepared nps of manganese ferrites in 4:1 (w/w) were taken in dried mortar after adding a few drops of paraffin oil; it was crushed by pastel to prepare the invariable mixture. A capillary glass tube (2 mm, i.d.) is filled with a homogeneous paste and a metal rod was used to pack it tightly. The backside of the capillary tube received a Pt wire inserted to complete the circuit. The same method was adopted to fabricate of bare GP electrode. The Al_2O_3 slurry (0.3 mM and 0.05 mM) were utilized to wash the electrode. Rinsing of the electrode with ethyl alcohol and drying in an N_2 atmosphere was adopted before the experiment.

2.4. Apparatus and measurement

The characterization of prepared nanocomposites was performed by the Panalytical X-ray diffractometer (XRD), model no. X'PertPRO, (Netherlands) with Cu K-alpha radiation (λ=1.5406Å), Hitachi SU-8010 "field emission scanning electron microscope" (FESEM), and "transmission electron microscope" (TEM) model (FP 5032/21 Tecnai G2 30 S-TWIN (serial No. 9921621/D934) Model No. 943205032211 made in the Czech Republic). Autolab Potentiostat/Galvanostate 101 (Netherlands) with three electrodes was used for all electrochemical analysis. All the electrochemical studies were carried out in a phosphate buffer solution of pH 5.0 with 0.1 M concentration at 25±2 ºC. The scan rate for CV and DPV were maintained as 100 mVs^{-1} & 50 mVs^{-1} respectively, maintaining voltage range from

0.2 to 0.8 V for UA and 0.7 to 1.3 V for GU for CV experiments. During the estimation of UA and GU in a mixture using prepared ($MnFe_2O_4$/GP) electrode, 0.2 to 1.4 V for CV & DPV experiments was continued.

3. RESULTS AND DISCUSSION

3.1. XRD analysis of manganese ferrite nano-composites

The X-ray powder diffraction (XRD) technique was employed to determine phase purity and crystal structure of nanocomposite. "Debye–Scherrer method" [22] was employed to evaluate the average crystallite size of nano-particles. The crystallite size of the prepared nanoparticles (D) was computed to be 12 to 14 nm. The value for a, b and c were observed 9.4000 A with a 90.0000° angle of α, β, and γ, hence the synthesized materials are cubic crystal.

3.2. FESEM and TEM study of manganese ferrite nano-composites

FESEM and TEM techniques were exploited to characterize size and morphology. Nano-composites having the particle size between 10-15 nm was found to possess cubic shape (mostly). Fig. 2(a) indicates the image of FESEM nano-composites and Fig. 2(b) represents the TEM image.

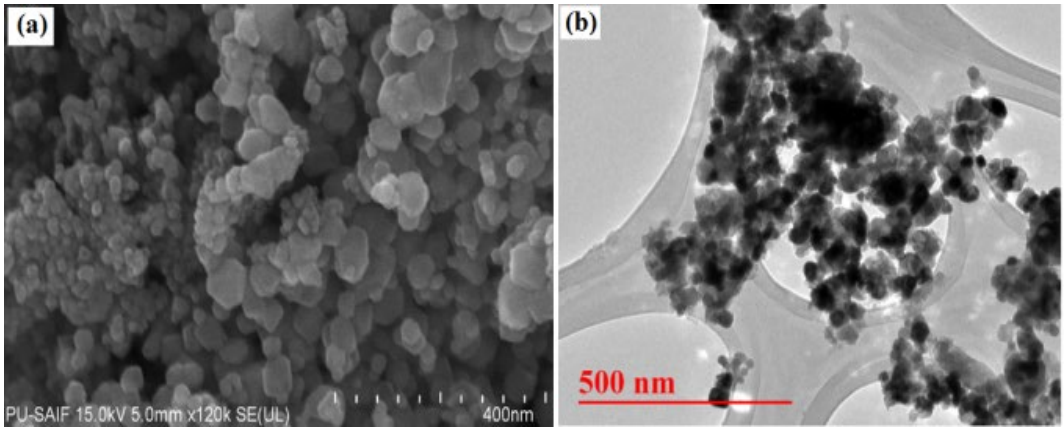

Fig. 2. (a) FESEM image and **(b)** TEM image of synthesized $MnFe_2O_4$ nano-particles

3.3. Electrochemical studies

A reference $[Fe(CN)_6]^{-4}/[Fe(CN)_6]^{-3}$ redox process was utilized to analyze the electrochemical behavior of new electrodes. The CV plots using bare GP and np$MnFe_2O_4$/GP electrodes for $K_4[Fe(CN)_6]$ solution are indicated in Fig. 3. The peak potential separation (ΔEp) value is responsible for the electron transfer at the working electrode. Velasco equation shows a low value of peak potential separation makes electron transfer more efficient [23].

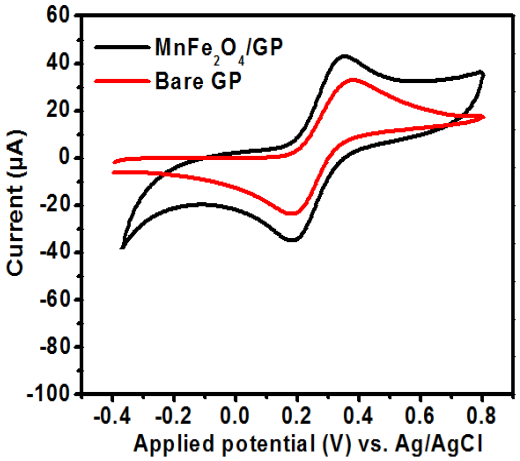

Fig. 3. CV plot at npMnFe2O4/GP and bare GP electrodes using K4[Fe(CN)6] redox system

ΔEp at both electrodes like npsMnFe2O4/GP and bare GP electrodes were 248 mV and 297 mV, respectively. The findings showed the npsMnFe2O4/GP electrodes improved electrochemical behavior in contrast with the bare GP electrode. It is interesting to note that, due to the reduced ΔEp (248 mV), made by the npsMnFe2O4/GP electrode showed increased sensor performance for UA and GU.

3.4. Electrochemical oxidation of UA and GU at npMnFe2O4/GP and bare GP electrodes

The sensor activity of the newly developed electrode was determined by CV and DPV technique towards UA & GU individually and in a mixture (Fig. 4).

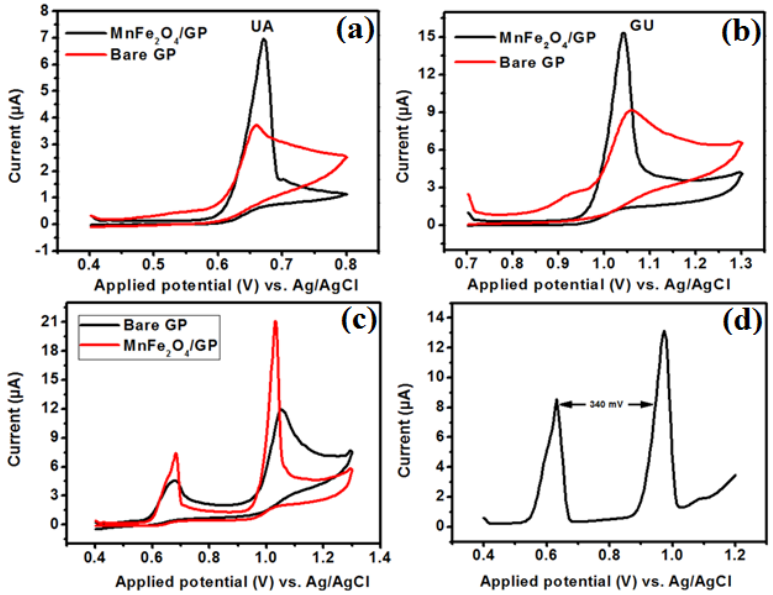

Fig. 4. CV plots of 0.1 mM UA **(a)**, 0.1 mM GU **(b)** at npMnFe2O4/GP electrodes (black) and bare GP electrode (red), CV plot **(c)** and DPV plot **(d)** in mixture of 0.1 mM UA and 0.1 mM GU at npMnFe2O4/GP electrode (using 0.1M phosphate buffer solution, pH 5.0; scan rate 100 mVs^{-1})

The cyclic voltammograms for uric acid and guanine individually at bare GP and npMnFe$_2$O$_4$/GP are shown in Fig. 4(a) and Fig. 4(b), respectively Fig. 4(c) and Fig. 4(d) represented the CV and DPV plot, respectively in the mixture of UA and GU. UA & GU exhibited irreversible oxidation characters at bare GP and npMnFe$_2$O$_4$/GP electrodes.

The oxidation peak potential of npMnFe$_2$O$_4$ / GP electrodes is 673 mV and 1045 mV for UA and GU respectively, while at bare GP 653 mV & 1056 mV, respectively. All the CV calculations were performed by maintaining scan rate-100 mV s^{-1}, and DPV experiment conducted at scan rate -50 mVs^{-1}, step potential -5 mV, modulation amplitude -40 mV, modulation time -0.02 s and interval time -0.1 s.

3.5. Effect of pH and scan rate

Supporting electrolyte since having a pivotal role in the oxidation of biomolecule, the pH effect on UA & GU was studied using the phosphate buffer solution of 0.1 M concentration, by changing pH from 4.0 to 7.0. From the experiments, it was observed that any increment in pH of supporting electrolyte would shift the oxidation peak potential value negatively for both bio-molecules. The peak current was maximum at pH 5.0 and it decreased with further increment in pH (fig. 5(a), which might be because the biomolecules did have multi basic character [24, 25]. The impacts of scan rate on UA & GU oxidation have also been investigated by adjusting the scan rate from 5 to 500 mVs^{-1} . Newly prepared npMnFe$_2$O$_4$/GP electrodes the linear increment in peak current was presented in Fig. 5(b) and Fig. 5(c)).

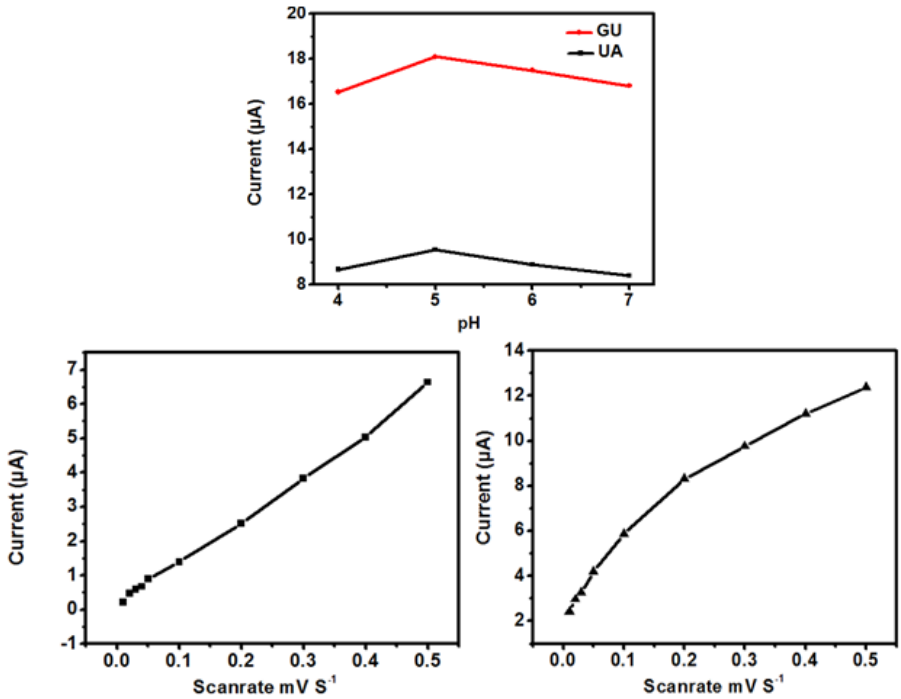

Fig. 5. (a) pH variation vs. current plot in phosphate buffer solution from pH 4 to pH 7and scan rate variation from 5 to 500 mVs^{-1} **(b)** for UA **(c)** GU at MnFe$_2$O$_4$/GP electrode

3.6. Simultaneous estimation of UA & GU

To determine UA & GU simultaneously at the npMnFe$_2$O$_4$/GP electrode, optimum CV experiments were performed at the preliminary stage. DPV experiment gave a higher peak current density and better resolution. Therefore, for the simultaneous determination and to know the linearity range of both molecules (UA & GU), a regulated DPV experiment by altering voltage from 0.4 V to 1.4 V was carried out. The linearity range of UA & GU, at npMnFe$_2$O$_4$/GP electrodes, was checked by keeping the concentration of one molecule fixed and changing the other. Fig. 6(a) and 6(b). The results revealed the linear increase of oxidation peak current with a conc. of UA and GU. The first linearity range for UA was observed from 1µM to 40 µM (IUA) y = 0.002UA + 0.082(R^2 = 0.890) and second linearity range was observed from 40 µM to 140 µM (IUA) y= 0.001UA + 0.132(R^2 = 0.975).

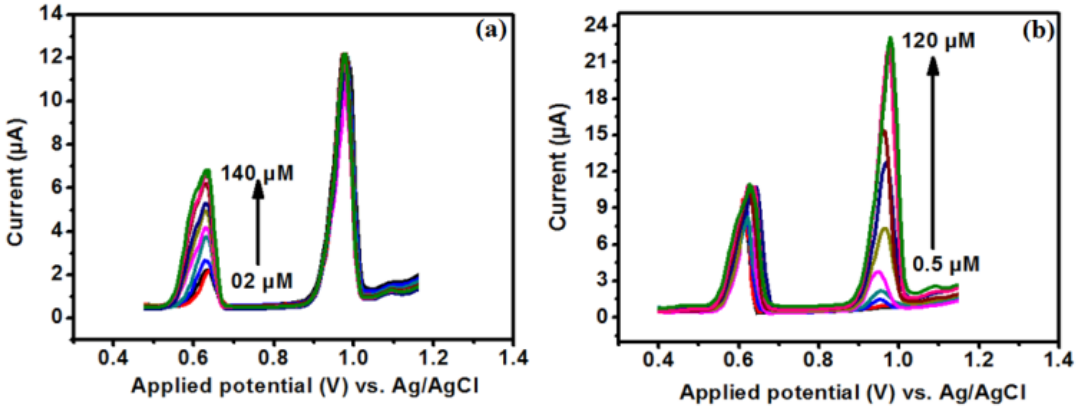

Fig. 6. (a) The concentration of UA in the range 1 - 140 µM at npMnFe$_2$O$_4$/GP electrode by holding the concentration of GU constant as 100 µM **(b)** GU varied from 0.5 - 120 µM at npMnFe$_2$O$_4$/GP electrode by holding the concentration of UA constant as 100 µM using 0.1M phosphate buffer solution with pH 5.0

The first linearity range for GU was observed from 0.5µM to 40 µM (I_{GU}) y = 0.015$_{GU}$ - 0.001(R^2=0.942) and second linearity range was observed from 40 µM to 100 µM (I_{GU}) y = 0.009$_{GU}$ + 0.272(R^2 = 0.996). The lower detection limits were recorded to be 400 & 450 nM for GU & UA respectively at the newly developed electrode.

3.7. Comparative study with previously developed electrode

Based on comparison with previously developed electrode it can be concluded that the newly developed electrode (npMnFe$_2$O$_4$/GP, modified graphite paste) had a better detection limit as well as linearity range. The limit of detection at npMnFe$_2$O$_4$/GP, modified graphite paste electrode was observed 400 and 450 nM with the linearity range 0.5 to 100 µM and 1 to 140 µM for GU and UA respectively. The results are summarized in Table 1.

3.8. Stability, Repeatability, reproducibility and sensitivity of the prepared electrode

To assess the stability of the prepared electrode, the electrode was kept at 30 ºC ± 1ºC for 30 days and retention in sensing capacity was observed more than 95 % as compared to the initial value. For repeatability, no noticeable change in sensitivity was observed on 10 times repetition of the experiment. Reproducibility has been checked by preparing five electrodes of npMnFe$_2$O$_4$/GP and utilized to verify sensitivity for the detection of these molecules and found to produce an almost similar response. The results suggested the electrode to have good stability, reproducibility, and sensitivity.

Table 1. Comparison of the developed electrode with literature reports

Electrodes	Guanine		Uric acid		Ref.
	Linear range (µM)	Detection limit (nM)	Linear range (µM)	Detection limit (nM)	
TAN-Ag NP-PANF/CPE	0.9-140	3000	-	-	[26]
PANI/MnO_2/GCE	10-100	4800	-	-	[27]
p-PTSA/GCE	10-100	350	10-100	5880	[28]
Pimox GO/GCE	3.3-103.3	480	3.6-249.6	590	[29]
UO x-poly(4-ASA)-PB-CSPE			10–200	3000	[30]
GO/Fe_3O_4@SiO_2/CSPE	-	-	0.75–300	570	[31]
npMnFe$_2$O$_4$/GP	0.5-120	400	02–140	450	Our method

Table 2. Validation parameters of the prepared electrodes

Electrode	Sample	Original/ Diluted sample (µM)	Spiking (µM)	Found (µM)	R.S.D[1] (%)	Recovery[2] (%)
MnFe$_2$O$_4$/GP nps	**Urine Sample**					
	UA	20	30	50.5	1.92	100.4
	GU	0	50	50.1	1.54	100.2
	Human serum sample					
	UA	20	30	49.8	1.4	98.8
	GU	0	50	50.3	1.7	99.3

[1]Relative standard deviation

[2]Recovery $= \frac{\text{Found}(\mu\text{M})\text{-Diluted biological fluids/pharmaceutical sample}(\mu\text{M})}{\text{Spiking}(\mu\text{M})} \times 100\%$

3.9. Analysis of real sample using $MnFe_2O_4$/GP modified electrode

The efficiency of the prepared working electrodes in the real sample was investigated in urine & human serum samples. Samples underwent centrifugation at four thousand rpm followed by a collection of the sample by dropper and finally suitably diluted. 100.4 & 98.8% were the recovery value of UA in urine and serum samples respectively indicating that developed electrode can be used for clinical diagnosis.

4. CONCLUSION

This article contains the simple synthesis procedure for manganese ferrite nano-composite. The synthesized material has a cubic structure with size ranging from 12-14 nm as characterized by XRD, FESEM, and TEM techniques. A graphite paste based electrode was fabricated with these materials and used as an electrochemical sensor to detect UA & GU in bio-fluids separately and in combination. The voltammetric techniques like CV & DPV were used for the electrochemical measurements of these molecules. The $MnFe_2O_4$ /GP electrodes showed remarkable results and succeeded to determine UA and GU with a limit of 450 and 400 nM respectively. The easy synthesis procedure and surpassing sensitivity are the leading merits of the modified electrode to make it suitable for use in clinical diagnosis and pharmaceutical research .

ACKNOWLEDGMENT

The authors are thankful to GLA University, Mathura (India), and Jadavpur University, Kolkata (India) for all kinds of support related to the work.

REFERENCES

[1] G. A. Evtugyn, R. V. Shamagsumova, R. R. Sitdikov, I. I. Stoikov, I. S. Antipin, M. V. Ageeva, and T. Hianik, Electroanal. 23 (2011) 2281.
[2] R. A. Wise, Nature Rev. Neurosci. 5 (2004) 483.
[3] P. B. Wood, P. Schweinhardt, E. Jaeger, A. Dagher, H. Hakyemez, E. A. Rabiner, M. C. Bushnell, and B. A. Chizh, Euro. J. Neurosci. 25 (2007) 3576.
[4] S. Červenka, S. E. Pålhagen, R. A. Comley, G. Panagiotidis, Z. Cselényi, J. C. Matthews, R. Y. Lai, C. Halldin, and L. Farde, Brain 129 (2006) 2017.
[5] Z. Dursun, and B. Gelmez, Electroanalysis 22 (2010) 1106.
[6] Z. Yang, X. Huang, J. Li, Y. Zhang, S. Yu, Q. Xu, and X. Hu, Microchim. Acta. 177 (2012) 381.
[7] S. H. Kollins, and R. A. Adcock, Prog. Neuro-Psychoph. 52 (2014) 70.
[8] M. E. Rice, Trends Neurosc. 23 (2000) 209.
[9] N. Lavanya, C. Sekar, R. Murugan, and G. Ravi, Mater. Sci. Eng. C 65 (2016) 278.

[10] A. Yari, and S. Derki, Sens. Actuators B Chem. 227 (2016) 456.
[11] J. Li, J. Jiang, H. Feng, Z. Xu, S. Tang, P. Deng, and D. Qian, RSc Adv. 6 (2016) 31565.
[12] H. Wang, F. Ren, C. Wang, B. Yang, D. Bin, and K. Zhang, RSc Adv. 4 (2014) 26895.
[13] S. Pradhan, R. Das, S. Biswas, D. K. Das, R. Bhar, R. Bandyopadhyay, and P. Pramanik, Electrochim. Acta. 238 (2017) 185.
[14] S. Pradhan, S. Biswas, D. K. Das, R. Bhar, R. Bandyopadhyay, and P. Pramanik, New J. Chem. 42 (2018) 564.
[15] R. Chokkareddy, N. K. Bhajanthri, and G. G. Redhi, Indian J. Chem. (2018) 887.
[16] Y. Kumar, S. Pradhan, S. Pramanik, R. Bandyopadhyay, D. K. Das, and P. Pramanik, J. Electroanal. Chem. 830 (2018) 95.
[17] Y. Kumar, P. Singh, P. Pramanik, and D. Das, J. Sci. Ind. Res. 78 (2019) 177.
[18] Y. Kumar, P. Pramanik, and D. K. Das, Heliyon 5 (2019) e02031.
[19] K. Sihombing, M. C. Tamba, W. S. Marbun, and M. Situmorang, Indian J. Chem. 57 (2018) 175.
[20] Y. Kumar, V. K. Vashishtha, and D. K. Das, Lett. App. NanoBioscience 9 (2020) 866.
[21] Y. Kumar, V. K. Vashishtha, Singh, P. P. A. Kumar, and D. K. Das, Biointerface Res. Appl. Chem. 10 (2020) 5855.
[22] B. C. Deceased, and S. Stock, Elements of X-ray Diffraction. Prentice Hall Upper Saddle River, NJ, USA (2001).
[23] X. Zhang, S. Duan, X. Xu, S. Xu, and C. Zhou, Electrochim. Acta. 56 (2011) 1981.
[24] W. Sun, J. Liu, X. Ju, L. Zhang, X. Qi, and N. Hui, Ionics 19 (2013) 657.
[25] B. Rezaei, H. Khosropour, A. A. Ensafi, M. Dinari, and A. Nabiyan, RSC Adv. 5 (2015) 75756.
[26] A. Yari, and M. Saidikhah, J. Electroanal. Chem. 783 (2016) 288.
[27] Y. Hui, X. Ma, X. Hou, F. Chen, and J. Yu, Ionics 21 (2015) 1751.
[28] S. Jesny, S. Menon, and K. G. Kumar, RSC adv. 6 (2016) 75741.
[29] X. Liu, L. Zhang, S. Wei, S. Chen, X. Ou, and Q. Lu, Biosens. Bioelectron. 57 (2014) 232.
[30] F. S. da Cruz, F. de Souza Paula, D. L. Franco, W. T. P. dos Santos, and L. F. Ferreira, J. Electroanal. Chem. 806 (2017) 172.
[31] H. Beitollahi, F. G. Nejad, and S. Shakeri, Anal. Methods 9 (2017) 5541.